

# Learning About Learning: A Physics Path from Spin Glasses to Artificial Intelligence

Denis D. Capriotti,\* Matheus Haas,\* Constantino F. Vasconcelos, and Mauricio Girardi-Schappo†

*NeuroPhysics Laboratory,  
Departamento de Física,  
Universidade Federal de Santa Catarina, Florianópolis SC,  
Brazil. 88040-900*

(Dated: January 13, 2026)

The Hopfield model, originally inspired by spin-glass physics, occupies a central place at the intersection of statistical mechanics, neural networks, and modern artificial intelligence. Despite its conceptual simplicity and broad applicability – from associative memory to near-optimal solutions of combinatorial optimization problems – it is rarely integrated into standard undergraduate physics curricula. In this paper, we present the Hopfield model as a pedagogically rich framework that naturally unifies core topics from undergraduate statistical physics, dynamical systems, linear algebra, and computational methods. We provide a concise and illustrated theoretical introduction grounded in familiar physics concepts, analyze the model’s energy function, dynamics, and pattern stability, and discuss practical aspects of simulation, including a freely available simulation code. To support instruction, we conclude with classroom-ready example problems designed to mirror research practice. By explicitly connecting fundamental physics to contemporary AI applications, this work aims to help prepare physics students to understand, apply, and critically engage with the computational tools increasingly central to research, industry, and society.

## I. INTRODUCTION

Back in the 1980’s, Hopfield (Hopfield, 1982, 1984) introduced a neural network for associative memory. Just as if it were magic, given some input, the network evolved to retrieve an associated pattern that was encoded in the connections between neurons. This idea was inspired by the physics of spin glasses and still constitutes the basic paradigm for memory encoding in the brain today (Rolls and Treves, 1999, 2024). It can also be applied to compute near-optimal solutions (Hopfield and Tank, 1985, 1986) for complex combinatorial problems by mapping a cost function to the network’s Hamiltonian (Hertz *et al.*, 1991; Rojas, 1996). These discoveries lead John Hopfield to share with Geoffrey Hinton (whose work focused on Boltzmann machines (Ackley *et al.*, 1985; Hinton and Sejnowski, 1983)) the 2024 Nobel Prize in Physics (Nobel Prize Outreach, 2024).

Neural networks have rapidly evolved from specialized academic tools into widely deployed technologies central to data analysis, artificial intelligence (AI), and decision making. This has increased the demand for physicists in both research and industry who are literate in applying physical knowledge and reasoning to computational tools that can solve problems. Although undergraduate physics provides many of the necessary conceptual foundations, these ideas are often taught in isolation

and without explicit connection to contemporary applications, making it difficult for students to recognize their relevance beyond the classroom.

The Hopfield model provides a compact and pedagogically rich example in which these connections can be made explicit. Here, we show how core undergraduate ideas from statistical physics, computational methods, dynamical systems, and linear algebra arise together in a simple model and useful tool. The more suitable placement for the model is in courses that teach computational methods in Physics. At the end of the paper, we give a set of classroom-ready example problems that can guide instructors when approaching this subject. We wrote them in a way to emulate research practice.

Given its inherent interdisciplinarity, it is not covered in standard physics’ textbooks, only in books for specialized audience (Hertz *et al.*, 1991; Peretto, 1994; Rojas, 1996). Thus, we give a fundamental but brief and illustrated account of the theory that explains the workings of the Hopfield network using concepts from the standard curriculum.

Section II reviews the statistical physics of the Ising magnet and spin glasses. In Section III, we introduce the Hopfield model and use ideas from spin-glass theory to guide the construction of its energy function, showing how equilibrium states can be controlled by encoding memory patterns (*i.e.*, training the network – Section III.A). Then, we introduce the Hopfield dynamics (Section III.B), and study the stability of these equilibria (Section III.C). We also discuss how to simulate the model in Section III.D, and provide a fully functional code made freely available (Girardi-Schappo *et al.*, 2025).

\* These authors contributed equally to this work

† Corresponding author; [girardi.s@gmail.com](mailto:girardi.s@gmail.com)

Finally, Section IV presents examples of how to bring significance to different Physics undergraduate courses through the Hopfield model.

## II. STATISTICAL PHYSICS: ISING FERROMAGNET AND SPIN GLASS

Spin glasses are a thermodynamic magnet state made from random and frustrated pairwise interactions between spins, where the material is organized in random spatial domains of different magnetization (Edwards and Anderson, 1975; Sherrington and Kirkpatrick, 1975). The question: “what macroscopic states form from a given set of microscopic interactions?” is actually answered by the Hopfield model. Even though before it, there were solvable models of spin glasses (Nishimori, 2001), physicists were not interested in exactly *which* states are obtained in a spin glass, only how many of these states there are, and if these states *can* be obtained (Mézard *et al.*, 1987).

This was the study of the thermodynamic properties of these objects. In contrast, Hopfield then offered a simple recipe for connecting microscopic interactions with the observable macroscopic state – something that is under the umbrella of *unsupervised learning* in nowadays AI jargon. In doing so, he inescapably offered an insight into how memories can be encoded in the brain, and how we can perform complex tasks, such as pattern completion or separation (*i.e.*, recognizing something or distinguishing between things from incomplete information) (Hopfield, 1982; Rolls and Treves, 1999, 2024).

Often introduced as a simplified neural network, the model is still fundamental in Neuroscience and Computer Science research (Gerstner *et al.*, 2014; Rojas, 1996; Rolls and Treves, 1999, 2024). It is formally equivalent to an Ising magnet with appropriately chosen spin interactions (Hertz *et al.*, 1991; Peretto, 1994; Rojas, 1996). At the same time, the process of matching an incomplete input to a memory can be explained by a high-dimensional dynamical system whose evolution converges toward fixed points (global or local equilibrium states).

Surprisingly, this convergence is guaranteed by the construction of the pairwise interactions from simple elementary vector operations. This is the reason why this model bears different names, and is the paradigmatic example of the so-called attractor networks (Gerstner *et al.*, 2014; Rojas, 1996). Thus, we can understand it taking advantage of simple ideas that are typically introduced in undergraduate courses in Thermodynamics and Statistical Physics, Computational Physics, Dynamical Systems, and Linear Algebra. Each of these provide a complementary view of the same underlying object.

In this section, we want to analyze the relation between the parameters of the Ising model and the equilibria (minimum energy states) of the system. So that later,

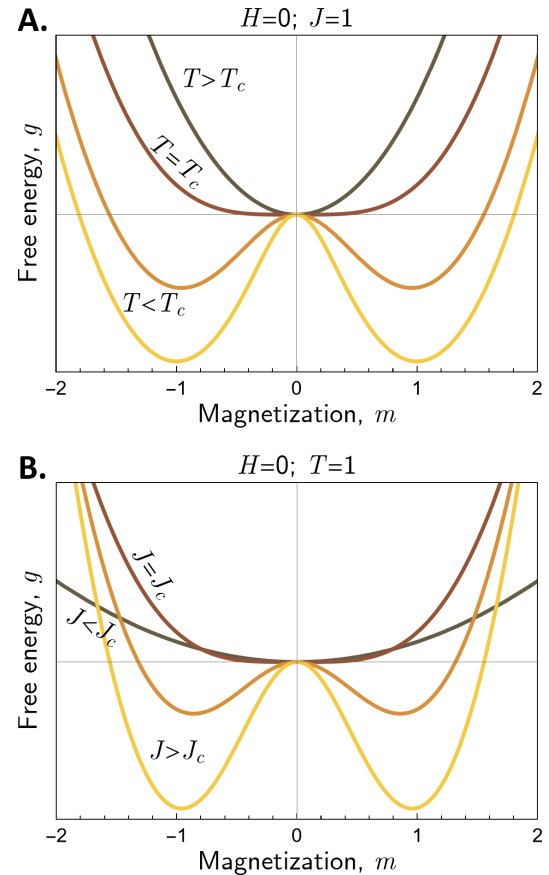


FIG. 1 **Ising ferromagnet free energy functional.** Plots of Eq. (5) using units in which  $k_B = 1$ . The minima of  $g$  are the thermodynamic (observable) states of the system. **A.** Break of symmetry as  $T$  decreases with fixed  $J = 1$ : the equilibrium  $m = 0$  ( $T > T_c = 1$ ) splits into  $m = \pm m_0$  for  $T < T_c$ ; both are solutions to the equation of state, Eq. (2). **B.** A similar break of symmetry happens for fixed  $T = 1$ , but changing  $J$  around  $J_c = 1/T = 1$ . Although  $J$  is an effective interaction between spins and cannot be changed in real magnets, it also controls the thermodynamic (equilibrium) states; this is the fundamental feature explored by Hopfield.

we can extend this reasoning to understand the Hopfield network.

### A. Mean-field theory of ferromagnets

We start from a system that is usually approached in standard introductory courses in undergraduate statistical physics: the Ising paramagnet made of  $N$  spins. Its Hamiltonian is a function of the system state described by the column vector  $\vec{\sigma} = [\sigma_1 \cdots \sigma_N]^T$ , ( $T$  for transpose)

$$\mathcal{H}(\vec{\sigma}) = -H \sum_{i=1}^N \sigma_i , \quad (1)$$

where  $H$  is an external magnetic field in suitable units (*e.g.*, in terms of the Bohr magneton and the gyro-magnetic constant) and the spin variables can be  $\sigma_i =$

$\pm 1$  (Salinas, 2001). Defining the inverse temperature,  $\beta = 1/(k_B T)$ , where  $k_B$  is the Boltzmann constant, the canonical partition function  $Z = [2 \cosh(\beta H)]^N$  yields the (dimensionless) equation of state for the magnetization per spin,  $m = \tanh(\beta H)$ . This system is not very exciting: the magnetization is always a direct response to the applied magnetic field: if  $H > 0 (< 0)$ , then  $m > 0 (< 0)$ ; otherwise,  $H = 0$  gives no spontaneous magnetization.

The ferromagnetic state can be created if we replaced  $H$  by an effective field,  $H_{\text{eff}} = H + Jm$ , where  $J > 0$  is the result of the spins' own magnetic influence on one another, giving the equation of state

$$m = \tanh(\beta J m + \beta H). \quad (2)$$

Now, even if  $H = 0$ , the equation  $m = \tanh(\beta J m)$  can have either one solution,  $m = 0$ , when  $\beta J < 1$ , or three solutions,  $m = 0$  and  $m = \pm m_0$ , when  $\beta J > 1$ . This is because the hyperbolic tangent is a sigmoid function bounded within  $(-1; +1)$ , with a slope of  $\tanh(\beta J m) \sim \beta J m + \mathcal{O}[m^2]$  near  $m = 0$ . Thus,  $\beta_c J = J/(k_B T_c) = 1$  is a phase transition with critical temperature  $T_c = J/k_B$ . For temperatures  $T > T_c$ , the system is a paramagnet, but for  $T < T_c$ , the system generates spontaneous magnetization and becomes a ferromagnet.

This is the Curie-Weiss mean-field theory of the Ising model (Salinas, 2001), and it can be made more rigorous if we started from the Hamiltonian in Eq. (1), replacing  $H$  by the effective field  $H_{\text{eff}} = \frac{J}{2N} \sum_j \sigma_j + H$ ,

$$\mathcal{H}(\vec{\sigma}) = -\frac{J}{2N} \sum_{i=1}^N \sum_{j=1}^N \sigma_i \sigma_j - H \sum_{i=1}^N \sigma_i, \quad (3)$$

where the factor  $1/2$  in front of the double sum is there to compensate the fact that all terms are being summed twice, since  $\sigma_i \sigma_j = \sigma_j \sigma_i$ . The Hamiltonian in Eq. (3) favors states in which  $\sigma_i$  and  $\sigma_j$  are aligned (*i.e.*, have the same sign). The canonical partition function can be written as (Carneiro *et al.*, 1989; Salinas, 2001)

$$Z = \left( \frac{N\beta J}{2\pi} \right)^{1/2} \int_{-\infty}^{+\infty} \exp(-\beta N g) dm, \quad (4)$$

where  $g \equiv g(T, H; m)$  is the Gibbs free energy functional

$$g(T, H; m) = \frac{J}{2} m^2 - \frac{1}{\beta} \ln(2 \cosh(\beta J m + \beta H)). \quad (5)$$

The minima of  $g(T, H; m)$  with respect to  $m$  are the thermodynamic states where we can observe the system (Fig. 1A). Minimizing Eq. (5), *i.e.*, finding  $m$  such that  $\partial g / \partial m = 0$ , leads to the magnetization in Eq. (2). The usual way to look at  $g$  is by keeping  $J$  fixed (since it results from the influence of other spins), and verify that the minima of  $g$  respond to changes in  $T$ . This is the typical scenario of the critical phase transition, often termed

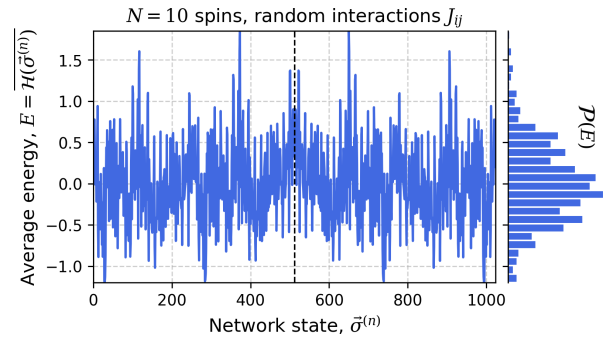


FIG. 2 **Average of the spin-glass Hamiltonian over the  $J_{ij}$  disorder.** The Hamiltonian in Eq. (6) was averaged over 100 realizations of the random matrix  $\mathbf{J}$  for all the  $2^N$  states of an  $N = 10$  spins system.  $J_{ij}$  was sampled from a Gaussian distribution with zero mean and unity standard deviation. Each network state  $\vec{\sigma}^{(n)}$  is assigned an index  $n$ , and is put on the horizontal axis (left). The energy fluctuates around  $\langle E \rangle = 0$  according to a Gaussian distribution as  $N \rightarrow \infty$  (right), motivating the random-energy models for spin glasses (Derrida, 1980; Ruelle, 1987). Dashed line marks the state  $n = 2^9 = 512$ : larger  $n$  are flipped states.

as “break of symmetry” because the single minimum in  $g$  for  $T > T_c$  splits into two for  $T < T_c$  (Fig. 1A).

If we let go of the fixed  $J$  constraint, and think of it as a free parameter, we see that the minima of  $g$  also respond to changes in  $J$  when  $T$  is fixed (Fig. 1B). This is the first fundamental principle that explains the functioning of Hopfield networks. Since  $J$  controls the thermodynamic state of the system, we naively expect that these minima must also be dynamically achievable when the spins change with time,  $\sigma_i(t)$ . Although not in general, this is expected at least in the case where the (stochastic) dynamics obey detailed balance, or for some particular deterministic temporal evolution (Hertz *et al.*, 1991; Peretto, 1994).

## B. Mean-field theory of spin glasses

There is no *a priori* physical requirement for the  $J$  to be homogeneous between every pair of spins. One can imagine that materials that contain impurities might result in different interactions between different pairs of spins. This is called *quenched disorder* (since it is fixed in time), and leads to the spin glass Sherrington-Kirkpatrick Hamiltonian (Sherrington and Kirkpatrick, 1975)

$$\mathcal{H}(\vec{\sigma}) = -\frac{1}{2} \sum_{i=1}^N \sum_{j=1}^N \frac{J_{ij}}{N} \sigma_i \sigma_j - H \sum_{i=1}^N \sigma_i. \quad (6)$$

We kept the  $1/2$  factor because we are assuming that  $J_{ij} = J_{ji}$ . As long as  $J_{ij}$  obeys a distribution with a well-defined average, and standard deviation that scales with  $1/\sqrt{N}$ , the replica method can be applied to Eq. (6) (Mézard *et al.*, 1987; Sherrington and Kirkpatrick, 1975). Frequently,  $J_{ij}$  is considered to be nor-

mally distributed around zero. Simply put, the replica method consists of evaluating  $\mathcal{H}(\vec{\sigma})$  for a given realization (or replica)  $\mu$  of the  $J_{ij}$  coupling matrix, resulting in a Helmholtz free energy  $f^{(\mu)}$ ; this procedure is repeated over and over again to obtain a mean free energy  $f = \overline{f^{(\mu)}}$ , where the bar denotes an average over the whole  $J_{ij}$  ensemble. Then, some thermodynamic properties can be derived in a self-consistent way from  $f$ . For illustration, we show in Fig. 2 the landscape for the average energy  $E = \overline{\mathcal{H}(\vec{\sigma})}$  over independent realizations of the  $\mathbf{J}$  matrix.

This leads to analytical expressions for the total magnetization,  $m$ , and for the Edwards-Anderson (Edwards and Anderson, 1975) order parameter,  $q_{\text{EA}}$ ,

$$q_{\text{EA}} = \overline{\frac{1}{N} \sum_{i=1}^N m_i^2}, \quad (7)$$

where  $m_i = \langle \sigma_i \rangle$  is the thermal average of spin  $i$  (local magnetization at site  $i$ ), and the bar denotes averaging of the whole expression over the ensemble of  $J_{ij}$  (Mézard *et al.*, 1987). A spin glass is defined as a low-temperature system where  $m = 0$ , but  $q_{\text{EA}} > 0$  (Sherrington and Kirkpatrick, 1975). In other words, even though the net magnetization is null, the system presents a random distribution of locally magnetized domains.

When decreasing the temperature of a spin glass starting from above the Curie temperature, the system will freeze in one particular state  $\mu$  out of possibly infinite ( $N \rightarrow \infty$ ) configurations  $\{m_i\}$  for the local magnetizations (Mézard *et al.*, 1984). This phase transition and the stability of these states is studied in terms of the overlap between them,

$$q^{(\mu,\nu)} = \overline{\frac{1}{N} \sum_{i=1}^N m_i^{(\mu)} m_i^{(\nu)}}. \quad (8)$$

Here,  $m_i^{(\mu)}$  is the local magnetization of site  $i$  corresponding to a given macroscopic state  $\mu$  (obtained from a particular sample of the matrix  $J_{ij}$ ). Treating the site-related variables as vectors,  $\vec{m}_i^{(\mu)} = [m_1^{(\mu)} \dots m_N^{(\mu)}]^T$ , the overlap is just the scalar product between two macroscopic (equilibrium) states.

When  $\nu = \mu$ ,  $q^{(\mu,\nu)} = q^{(\mu,\mu)} = q_{\text{EA}}$  (Mézard *et al.*, 1984), since the definition in Eq. (7) should not change from one realization of the  $J_{ij}$  to the other, so the averaging over the quenched disorder can be neglected (Mézard *et al.*, 1987). An analogous overlap will also be defined for the Hopfield model, and is crucial for deriving the Hopfield energy function, and verifying the convergence of the system towards an attractor (Peretto, 1994).

Spin glasses form the base for understanding Hopfield networks, but are also themselves part of contemporary research in Statistical Physics. So far, we offered an intuitive phenomenological account for the study of these

systems that can inspire classroom examples and discussion. In this context, one is interested in computing the usual thermodynamic properties of the spin glass, such as the susceptibility, magnetization, order parameter, or other critical exponents. The phase diagram including para, ferro and glass phases can also be traced (Mézard *et al.*, 1987; Sherrington and Kirkpatrick, 1975), but is out of the scope of our work.

### III. HOPFIELD NEURAL NETWORK: CONTENT-ADDREASABLE MEMORY

The fundamental question asked by Hopfield (Hopfield, 1982) is whether *content-addressable memory* can emerge from the collective interactions of many simple units (“neurons”). The human brain provides a compelling example of this capability: when presented with an incomplete or degraded image of a familiar face, we can often recognize the person almost immediately.

At first glance, it is straightforward to imagine a computer program that performs a similar task. Given a partial image as input, the program could search through a database and return the most similar stored image according to some chosen metric. Such an approach, however, relies on an exhaustive search through all items in the database. As the number of stored images increases, this procedure rapidly becomes inefficient.

This strategy is also fragile. If the input image differs in a systematic way from all stored examples – say, the person is wearing a hat, grew a beard, or got a scar – the program may fail entirely. In contrast, content-addressable memory in biological systems appears both efficient and robust: such features would not compromise our ability to quickly recognize the person. This raises the question of how such behavior can arise from simple interacting elements.

So far, we have identified two noteworthy features: (a) the coupling between spins can be directly related to the observable state of the system; and (b), when these couplings vary from pair to pair, the system admits states with zero net magnetization in which the spins are nevertheless frozen into a specific configuration.

This leads to a central question: can we deliberately encode these “frozen states” into the Hamiltonian? If so, one might expect that a stochastic dynamics obeying detailed balance would drive the system toward them (such as the Metropolis (Newman and Barkema, 1999) or Glauber (Tomé and Oliveira, 2015) Monte Carlo dynamics). Surely, these states would have to be recorded as minima of the Hamiltonian.

At this point, the discussion shifts from thermodynamics toward mechanics. Rather than focusing on the minimization of the free energy, our interest turns to the structure of the Hamiltonian itself and the states that minimize it. In other words, given an initial condition

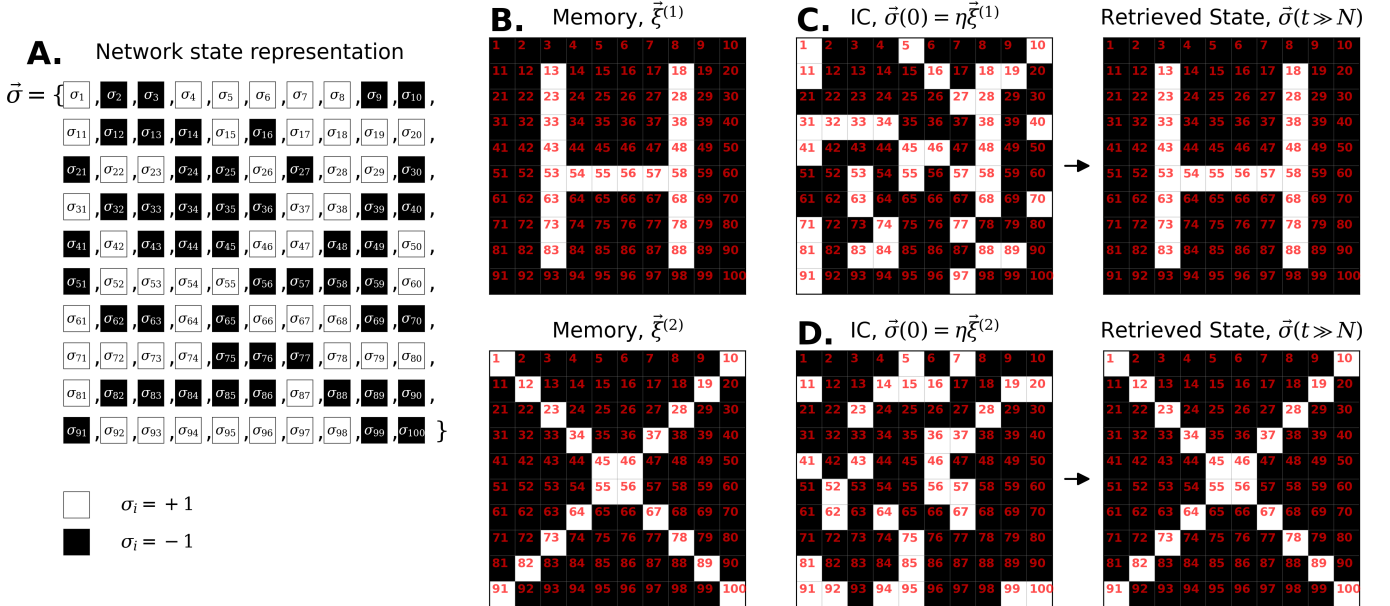


**FIG. 3 Retrieval of patterns.** **A.** The state vector  $\vec{\sigma}$  of a Hopfield network with  $N = 100$  neurons (“spins”) represented on a lattice of lateral size  $L = \sqrt{N} = 10$  for illustration. **B.** Two memories are stored in the network using Eq. (11); the number in each site is the index of the corresponding neuron forming either an “H” pattern, memory  $\vec{\xi}^{(1)}$ , or an “X” pattern, memory  $\vec{\xi}^{(2)}$ . **C.** Starting from a random IC near “H” (left), iterating the network converges to “H” (right). **D.** Starting from a random IC near “X” (left), iterating the network converges to “X” (right).

(IC)  $\vec{\sigma}(0)$ , say the incomplete error-prone face picture, the system would naturally flow toward the frozen state  $\vec{\xi}^{(\mu)}$  (the matching person) that is a local minimum of  $\mathcal{H}$  and is closest to  $\vec{\sigma}(0)$  (Fig. 3). Here, we should call  $\vec{\xi}^{(\mu)}$  a *memory* indexed by  $\mu$  out of a total of  $P$  memories (also called *patterns*).

This would provide a mechanism for a more “real-world” content-addressable memory, and also potentially result on softwares that do not rely just on exhaustive searches – so smarter (and more biological) artificial intelligence. Luckily for us, it is possible to do this.

### A. Constructing the energy function

The network is said to have  $N$  neurons. We introduce a variable  $x_i = 1$  if neuron  $i$  is actively firing action potentials, or spikes, so it can be interpreted as an intrinsic firing rate (Gerstner *et al.*, 2014). Otherwise,  $x_i = 0$  and the neuron  $i$  is silent. Biologically, a “silent” neuron can still be firing spikes, but this happens randomly and very sparsely in time. We can convert this behavior into our familiar spin framework by making  $\sigma_i = 2x_i - 1$ , giving  $\sigma_i = 1$  for active or  $-1$  for inactive. The microscopic state  $\vec{\sigma}$  is defined analogously to the Ising magnet,  $\vec{\sigma} = [\sigma_1 \dots \sigma_N]^T$  and is typically represented as a square lattice (Fig. 3A).

In this scenario, a memory  $\vec{\xi}^{(\mu)}$  is made of a subset of the  $N$  neurons firing together (Fig. 3B), while the remaining are silent. Also, note that the energy that we

are going to derive is not to be interpreted literally, as is the case for the Hamiltonian of magnets. It is just a mathematical construct that can be used to understand the collective behavior of neurons.

Many times, it is worth reducing the dimensionality of the system to get some intuition about what is happening. In our case, taking inspiration from the study of spin glasses, Eq. (8), we can reduce the dimensionality of the network microstate  $n$  using the overlap with memory  $\mu$ ,

$$M(\vec{\xi}^{(\mu)}, \vec{\sigma}^{(n)}) = \frac{1}{N} \vec{\xi}^{(\mu)} \cdot \vec{\sigma}^{(n)} = \frac{1}{N} \left( \vec{\xi}^{(\mu)} \right)^T \vec{\sigma}^{(n)} = \frac{1}{N} \sum_{i=1}^N \xi_i^{(\mu)} \sigma_i^{(n)}. \quad (9)$$

This is just the scalar product between  $\vec{\sigma}^{(n)}$  and  $\vec{\xi}^{(\mu)}$ , with the prefactor  $1/N$  to normalize  $M(\vec{\xi}^{(\mu)}, \vec{\sigma}^{(n)})$  (Fig. 4A). When  $M(\vec{\xi}^{(\mu)}, \vec{\sigma}^{(n)}) = \pm 1$ , we know that the network state matches exactly the memory  $\vec{\sigma}^{(n)} = \vec{\xi}^{(\mu)}$ , or the antimemory,  $\vec{\sigma}^{(n)} = -\vec{\xi}^{(\mu)}$ . This is due to the spin-flip symmetry of the system: only half of the  $2^N$  states are unique.

The internal energy of the ferromagnet is  $U = \langle \mathcal{H} \rangle = -\frac{1}{2} J N m^2 - H N m$ , where we used  $\langle \sum_{i,j} \sigma_i \sigma_j \rangle \approx N^2 m^2$  and  $\langle \sum_i \sigma_i \rangle = N m$ , ignoring correlations. Since  $-1 < m < 1$ ,  $U$  has minima at  $m = \pm 1$  when  $H = 0$ . This suggests that  $\mathcal{H} \sim -\frac{1}{2} N M^2$  (Fig. 4B), so we define (Hertz

et al., 1991; Peretto, 1994)

$$\mathcal{H} = -\frac{1}{2}N \sum_{\mu=1}^P \left( M(\vec{\xi}^{(\mu)}, \vec{\sigma}) \right)^2. \quad (10)$$

Using the overlap from Eq. (9) and expanding the squared sum,

$$\begin{aligned} \mathcal{H}(\vec{\sigma}) &= -\frac{1}{2}N \sum_{\mu=1}^P \left( \frac{1}{N} \sum_{i=1}^N \xi_i^{(\mu)} \sigma_i \right)^2 \\ &= -\frac{1}{2N} \sum_{\mu=1}^P \left[ \sum_{i=1}^N \sum_{j=1}^N (\xi_i^{(\mu)} \sigma_i)(\xi_j^{(\mu)} \sigma_j) \right] \\ &= -\frac{1}{2} \sum_{i=1}^N \sum_{j=1}^N \left( \frac{1}{N} \sum_{\mu=1}^P \xi_i^{(\mu)} \xi_j^{(\mu)} \right) \sigma_i \sigma_j. \end{aligned}$$

We define the interaction weight,

$$W_{ij} = \frac{1}{N} \sum_{\mu=1}^P \xi_i^{(\mu)} \xi_j^{(\mu)}, \quad (11)$$

to obtain a familiar energy function,

$$\mathcal{H}(\vec{\sigma}) = -\frac{1}{2} \sum_{i=1}^N \sum_{j=1}^N W_{ij} \sigma_i \sigma_j. \quad (12)$$

We can simplify it even more by separating the main diagonal terms and noting that  $(\xi_i^{(\mu)})^2 = (\sigma_i^{(\mu)})^2 = 1$ , so  $W_{ii} = P/N$

$$\begin{aligned} \mathcal{H}(\vec{\sigma}) &= -\frac{1}{2} \left( \sum_{i=j=1}^N \frac{P}{N} + \sum_{i \neq j}^N W_{ij} \sigma_i \sigma_j \right) \\ &= -\frac{P}{2} - \frac{1}{2} \sum_{i \neq j}^N W_{ij} \sigma_i \sigma_j. \end{aligned}$$

Since  $P$  is a constant, it can be neglected because it does not change the dynamics, leaving the simplified energy function:

$$\mathcal{H}(\vec{\sigma}) = -\frac{1}{2} \sum_{i=1}^N \sum_{\substack{j=1 \\ j \neq i}}^N W_{ij} \sigma_i \sigma_j. \quad (13)$$

The weight matrix defined by Eq. (11) is often called a generalized Hebbian rule (Hebb, 1942). In fact, it can be seen as the correlation of neurons  $i$  and  $j$  taken across all input patterns during the *training* of the neural network. Although this prescription is not intended to be a realistic model of the so-called *synaptic plasticity*, it provides a simple and analytically tractable way to construct the interaction matrix of the system. From a physical perspective, the couplings  $W_{ij} > 0$  act as effective interactions

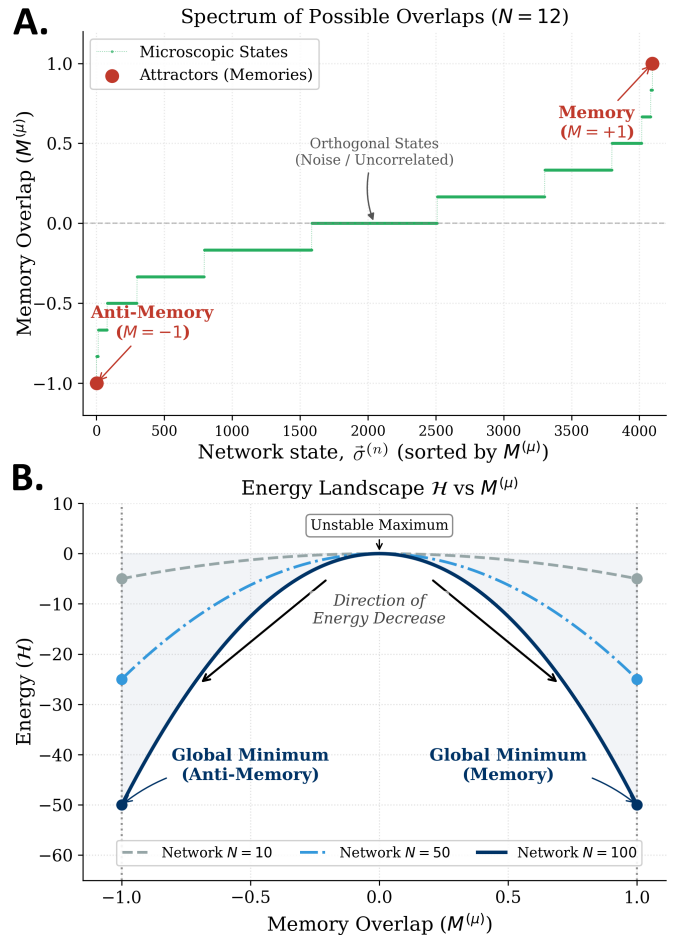


FIG. 4 **Overlap and Hopfield energy function.** **A.** Overlap between all  $2^{12}$  states and a single (random) memory pattern  $\vec{\xi}$  for a network with  $N = 12$  neurons, Eq (9). The microscopic states were sorted by their overlap value. The “staircase” structure reflects the discreteness of the system. Most of the states are uncorrelated with the memory,  $M \approx 0$ . The only states with  $M = \pm 1$  are the memory,  $\vec{\sigma}^{(n)} = \vec{\xi}$ , and antimemory,  $\vec{\sigma}^{(n)} = -\vec{\xi}$ . **B.** The inverted parabola, Eq. (10) for  $P = 1$ , is the simplest function that can be used to impose that  $M = \pm$  must be minima of  $\mathcal{H}$ . The arrows indicate the direction of energy decrease.

that favor the mutual alignment of “spins” in configurations corresponding to the memory; in Hebbian jargon: neurons that fire (spikes) together, wire (a synapse) together. Having  $W_{ij} < 0$  favors the “spins” pointing in opposite directions; or in biology, it means that the pair of neurons inhibit one another.

We can naturally get rid of  $P$  in the Hopfield Hamiltonian if we set  $W_{ii} = 0$ . This is not needed, but makes the model more robust (Hertz et al., 1991). Moreover, taking  $J_{ij} = N W_{ij}$ , this energy is analogous to that of the spin glass, Eq. (6), except that  $H = 0$  for the Hopfield model. Again, this is not a necessary condition for it to function properly, but gives it enhanced functionality. In fact, the energy in Eq. (13) can be generalized to

(already assuming  $W_{ii} = 0$ )

$$\mathcal{H}(\vec{\sigma}) = -\frac{1}{2} \sum_{i=1}^N \sum_{j=1}^N W_{ij} \sigma_i \sigma_j - \sum_{i=1}^N H_i \sigma_i , \quad (14)$$

where  $H_i$  is a local field, also known as the activation threshold of neuron  $i$  in the biological context.

Differently from the spin glass, though, we have derived a recipe, Eq. (11), that can be used to encode attractors in the Hamiltonian (Fig. 5). This is important for technological applications. Notice, however, that the  $W_{ij}$  definition is not unique. It does not work well for correlated memories (see Subsection III.C). In this case, one can use the pseudoinverse method (Hertz *et al.*, 1991) to calculate  $W_{ij}$  from the set of memories,  $\{\vec{\xi}^{(\mu)}\}$ .

Many dynamical systems are governed by a state function that either decreases during time evolution or must be extremized to reach a stable or optimal state. In dynamical systems theory, such a function is called a *Lyapunov function* (Strogatz, 2024). The same idea appears under different names in other fields, such as the Hamiltonian in statistical mechanics, the cost or objective function in optimization, and the fitness function in evolutionary biology.

This viewpoint is especially useful for constructing network models that have some technological application. If we can write down an energy function starting from Eq. (10), whose minimum represents the desired solution, then we can use the recipe given here to find the interaction strengths  $W_{ij}$  from the coefficients of the pairwise terms  $\sigma_i \sigma_j$  (see Section IV). Constant terms do not affect the dynamics, and terms linear in a single  $\sigma_i$  can be interpreted as thresholds or external fields. Higher-order terms involving three or more variables, however, cannot be represented within the present framework of pairwise interactions. Examples range from graph bipartitioning, the traveling salesman problem, the eight queens problem, the weighted matching problem, and diverse optimization problems in image processing (Hertz *et al.*, 1991; Rojas, 1996).

## B. Hopfield dynamics

For the model to perform memory matching with error correction, or any other task, the network state  $\vec{\sigma}$  must evolve in time toward a minimum in  $\mathcal{H}$ . Given an IC  $\vec{\sigma}(0)$  for a time step  $t = 0$ , we want the network to evolve to  $\vec{\sigma}(t \gg N) = \vec{\xi}^{(\mu)}$  for some stored pattern  $\mu$ . Although a formal treatment can be employed to justify the following dynamics (Peretto, 1994), we are going to introduce it phenomenologically, and then justify it by the minimization of the energy function.

Considering the network evolves in discrete time steps, we want to find a relation between  $\vec{\sigma}(t)$  and its next value,

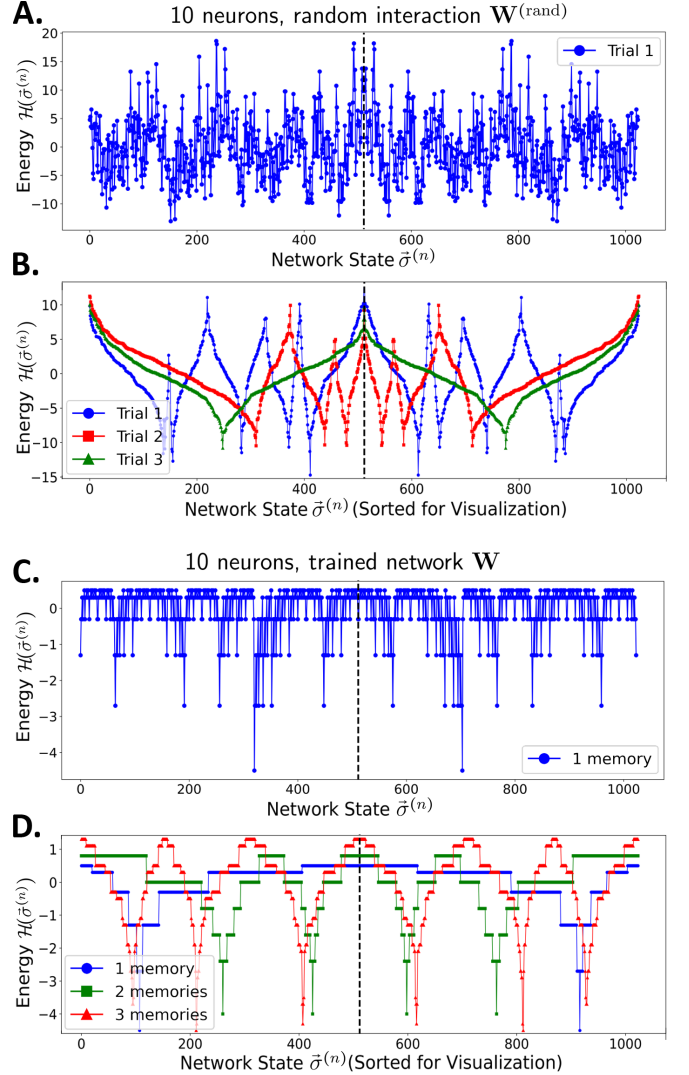


**FIG. 5 Hopfield energy landscape.** **A.** The Hopfield energy function, Eq. (13), for a network of  $N = 10$  neurons (“spins”) interacting through a random matrix  $\mathbf{W}$ ; it is exactly the same as the spin glass energy, Fig. 2. **B.** Three realizations of the random interaction energy, but network states  $\vec{\sigma}^{(n)}$  were grouped around the energy minima (network attractors) using Hamming distance, and then sorted according to their energy (decreasing when the state is to the left of the minimum, and increasing when the state is to the right of the minimum). Each realization results in an energy landscape with different attractors. **C.** Energy function with a single memory encoded using Eq. (11). **D.** Energy function with  $P = 1$ ,  $P = 2$  and  $P = 3$  encoded memories, with states sorted in the same way as in panel B. Spin-flip symmetry resulting from the definition, Eq. (10), makes the antimemory also an attractor.

$\vec{\sigma}(t+1)$ . Including the time-dependence and collecting the sums in  $i$  in Eq. (14),

$$\mathcal{H}(t) = -\frac{1}{2} \sum_{i=1}^N h_i(t) \sigma_i(t) , \quad (15)$$

where we defined

$$h_i(t) = \sum_{j=1}^N W_{ij} \sigma_j(t) + H_i \quad (16)$$

as the effective field acting on neuron  $i$ , and we absorbed the prefactor 2 into  $H_i$ , since it is an arbitrary constant.

Due to the minus sign in Eq. (15), both  $h_i(t)$  and  $\sigma_i(t)$  need to have the same sign to keep  $\mathcal{H}(t)$  negative. Otherwise,  $\mathcal{H}(t)$  is positive. This agrees with our intuition from the effective ferromagnet: the spin needs to be aligned with the effective field to minimize the free energy. So it is reasonable that the next state value  $\sigma_i(t+1)$  for neuron  $i$ , and  $h_i(t)$ , are aligned. The simplest way to do this is by taking  $\sigma_i(t+1) = \text{sign}[h_i(t)]$ , or, more generally,

$$\sigma_i(t+1) = F\left(\sum_{j=1}^N W_{ij} \sigma_j(t) + H_i\right), \quad (17)$$

where  $F(x) = \text{sign}(x)$  is the so-called transfer function defined by  $F(x \geq 0) = +1$ ;  $F(x < 0) = -1$ . Eq. (17) is analogous to the McCulloch-Pitts neuron, although  $F$  would have to be replaced by the Heaviside step function (Girardi-Schappo *et al.*, 2013; McCulloch and Pitts, 1943).

To confirm our suspicion, let us just update a single neuron  $k$  at random using Eq. (17), in any given time step, and calculate the energy shift,  $\Delta\mathcal{H}(t) = \mathcal{H}(t+1) - \mathcal{H}(t)$ . Using Eq. (15),

$$\Delta\mathcal{H}(t) = -\frac{1}{2} \left[ \sum_{i=1}^N h_i(t+1) \sigma_i(t+1) - \sum_{i=1}^N h_i(t) \sigma_i(t) \right].$$

Remember that  $W_{ii} = 0$ , so  $h_i(t+1) = h_i(t)$  for every neuron, and we are only updating neuron  $k$ , giving

$$\Delta\mathcal{H}(t) = -\frac{1}{2} \left[ h_k(t) \Delta\sigma_k(t) + \sum_{\substack{i=1 \\ i \neq k}}^N h_i(t) \Delta\sigma_i(t) \right],$$

where  $\Delta\sigma_i(t) = \sigma_i(t+1) - \sigma_i(t) = 0$  (for  $i \neq k$ ), leaving

$$\Delta\mathcal{H}(t) = -\frac{1}{2} h_k(t) \Delta\sigma_k(t). \quad (18)$$

Now, one of three updates could have happened: (a)  $\Delta\sigma_k(t) = 0$ , so the network did not change its state; (b)  $\Delta\sigma_k(t) = +2$  if neuron  $k$  switched from  $\sigma_k(t) = -1$  to  $\sigma_k(t+1) = +1$ , in which case  $h_k(t)$  must be positive, since  $\sigma_k(t+1)$  has the sign of  $h_k(t)$  due to the update rule in Eq. (17); or (c)  $\Delta\sigma_k(t) = -2$  if neuron  $k$  switched from  $\sigma_k(t) = +1$  to  $\sigma_k(t+1) = -1$ , in which case  $h_k(t) < 0$ . Thus, we have  $h_k(t) \Delta\sigma_k(t) > 0$  and  $\Delta\mathcal{H}(t) < 0$  for every update that changes the state of a neuron.

This proves that the energy decreases at every time step in which we update the state of the network using Eq. (17). Since this happens for one neuron at a

time, the network takes, on average,  $t \sim \mathcal{O}[N]$  time steps to go from the IC to the state where all neurons yield  $\Delta\sigma_k(t) = 0$  – and the network is said to have reached an attractor. So we define a “Monte Carlo” (MC) step as  $N$  time steps (Newman and Barkema, 1999); a MC step is also called an “epoch” in neural networks literature (Rojas, 1996).

Note that the update rule in Eq. (17) does not rely explicitly on the Hebbian prescription for  $W_{ij}$  in Eq. (11); it is therefore generally effective at finding minima of the energy function. While we have shown that the energy decreases during the dynamics, we must still ensure that, once a memory state  $\vec{\xi}^{(\mu)}$  is reached, it remains stable under further updates. In other words, applying Eq. (17) to  $\vec{\sigma}(t) = \vec{\xi}^{(\mu)}$  must result in  $\vec{\sigma}(t+1) = \vec{\xi}^{(\mu)}$ . This is the definition of an attractor, or a fixed point  $\vec{\sigma}^*$ , for discrete time systems (Strogatz, 2024),

$$\vec{\sigma}(t+1) = \vec{\sigma}(t) = \vec{\sigma}^*. \quad (19)$$

The Hebb construction guarantees that the intended memory states are minima of the energy. However, it can also inadvertently introduce other local minima when we try to store (sum) too many memories ( $P$  is large). These unintended minima are called *spurious memories*, and they do not correspond to stored patterns  $\vec{\xi}^{(\mu)}$ . As a consequence, the network is overloaded, becoming unreliable when retrieving a memory from incomplete inputs using the defined update rule. In practical terms, this would be analogous to recalling a random person when shown a familiar face. To avoid this problem, we need to limit the number of stored memories  $P$ .

### C. Pattern stability and storage capacity

For the model to be useful, the iteration of Eq. (17) must lead to one of the stored memories,  $\vec{\xi}^{(\mu)}$ . For a single memory,  $P = 1$ , it is simple to show that  $\vec{\xi}$  is an attractor, since  $W_{ij} = \frac{1}{N} \xi_i \xi_j$  and using  $\vec{\sigma}(t) = \vec{\xi}$ , we must retrieve  $\vec{\sigma}(t+1) = \vec{\xi}$ :

$$\begin{aligned} \sigma_i(t+1) &= F\left(\sum_{j=1}^N \left(\frac{1}{N} \xi_i \xi_j\right) \xi_j + H_i\right) \\ &= F\left(\xi_i \frac{1}{N} \sum_{j=1}^N (\xi_j)^2 + H_i\right) \\ &= F(\xi_i + H_i) = \xi_i, \end{aligned} \quad (20)$$

where we used  $\xi_j^2 = 1$  and assumed that  $H_i \in (-1; 1)$ . More clearly, if  $\xi_i = +1$ , then  $\xi \geq H_i$  for any  $H_i$  in the considered range; or else, if  $\xi_i = -1$ , then  $\xi_i < H_i$  for any  $H_i$  in the same range. The reasoning still stands if we analyze  $-\vec{\xi}$  instead, making it also a valid attractor.

The situation is more delicate when more memories are present. Considering we have  $P$  memories, let us test whether a given memory  $\nu$  can be retrieved:

$$\begin{aligned}\sigma_i(t+1) &= F\left(\sum_{j=1}^N \left(\frac{1}{N} \sum_{\mu=1}^P \xi_i^{(\mu)} \xi_j^{(\mu)}\right) \xi_j^{(\nu)} + H_i\right) \\ &= F\left(\frac{1}{N} \sum_{\mu=1}^P \xi_i^{(\mu)} \left(\sum_{j=1}^N \xi_j^{(\mu)} \xi_j^{(\nu)}\right) + H_i\right).\end{aligned}$$

Just as before, we can use the fact that when  $\mu = \nu$ , we have a term  $(\xi_j^{(\nu)})^2 = 1$  in the inner sum. So, we separate this term from the sum over patterns,

$$\begin{aligned}\sigma_i(t+1) &= F\left(\xi_i^{(\nu)} \frac{1}{N} \sum_{j=1}^N (\xi_j^{(\nu)})^2\right. \\ &\quad \left. + \frac{1}{N} \sum_{\substack{\mu=1 \\ \mu \neq \nu}}^P \xi_i^{(\mu)} \left(\sum_{j=1}^N \xi_j^{(\mu)} \xi_j^{(\nu)}\right) + H_i\right),\end{aligned}$$

giving

$$\sigma_i(t+1) = F\left(\xi_i^{(\nu)} + \kappa_i^{(\nu)} + H_i\right), \quad (21)$$

where we defined the crosstalk term,

$$\kappa_i^{(\nu)} = \sum_{\substack{\mu=1 \\ \mu \neq \nu}}^P \xi_i^{(\mu)} \left[ \frac{1}{N} \sum_{j=1}^N \xi_j^{(\mu)} \xi_j^{(\nu)} \right]. \quad (22)$$

Note that if  $\kappa_i^{(\nu)} \approx 0$ , Eq. (21) reduces to Eq. (20), and  $\sigma_i(t+1) = \sigma_i(t) = \sigma_i^* = \xi_i^{(\nu)}$ , as desired. Also, the term in brackets is the overlap (or rather the correlation) between memories  $\mu$  and  $\nu$ ,  $\frac{1}{N} \vec{\xi}^{(\mu)} \cdot \vec{\xi}^{(\nu)}$ . This explains why the derived weight, Eq. (11), requires that memories be uncorrelated: so that  $\kappa_i^{(\nu)}$  is small, and the network can properly recall its memories. The crosstalk depends only on the memories, so we can use Eqs. (21) and (22) to estimate the number of memories  $P$  that can be stored in the network – the storage capacity,  $P_{\max}$ .

First, let us write Eq. (21) more conveniently, defining  $C_i^{(\nu)} = -\xi_i^{(\nu)}(\kappa_i^{(\nu)} + H_i)$ ,

$$\sigma_i(t+1) = F\left(\xi_i^{(\nu)} - \frac{C_i^{(\nu)}}{\xi_i^{(\nu)}}\right) = F\left(\frac{1 - \xi_i^{(\nu)} C_i^{(\nu)}}{\xi_i^{(\nu)}}\right),$$

such that if  $C_i^{(\nu)} > 1$ , then the neuron state flips even when it starts from  $\xi_i^{(\nu)}$ , making  $\sigma_i$  unstable. This does not ruin the entire dynamics, but will leave at least one mistake on the recalled memory.

Considering that patterns are random, and that  $N > P \gg 1$ , the crosstalk term is a sum of approximately  $NP$

independent random numbers, each of which is  $+1$  or  $-1$ . In this case,  $C_i^{(\nu)}$  follows a binomial distribution that can be further approximated by a Gaussian with zero mean and variance  $P/N$ . This is due to large  $NP$ , and to the Central Limit Theorem. Thus, we can estimate the error probability  $P_{\text{err}}$  as the probability that  $C_i^{(\nu)} > 1$ ,

$$\begin{aligned}P_{\text{err}} &= \mathcal{P}(C_i^{(\nu)} > 1) = \sqrt{\frac{N}{2\pi P}} \int_1^\infty e^{-x^2 N/(2P)} dx \\ P_{\text{err}} &= \frac{1}{2} \left[ 1 - \text{erf}\left(\sqrt{N/(2P)}\right) \right]. \quad (23)\end{aligned}$$

Thus, to get  $P_{\text{err}} < 1\%$  (*i.e.* 1% os mistakes in the recalled pattern), the maximum number of patterns is  $P_{\max} = 0.15N$ . This is the original estimation by Hopfield (Hopfield, 1982). Although having  $P > 0.138N$  can already make a single neuron unstable state flip and propagate throughout the network, creating an avalanche of other flips and ruining the entire recall process. The reader is redirected to (Hertz *et al.*, 1991, Chapter 2) for more details.

## D. Simulation

The iteration of Eq. (17) can be made *synchronously*, updating all neurons simultaneously at each time step  $t$ , or *asynchronously*, updating one neuron at a time. The latter strategy is also called *sequential update*. In the previous subsection, we showed the conditions for convergence of the asynchronous case. The synchronous case can speed-up convergence to an attractor, but when  $H_i = 0$ , it can generate not only fixed points, but also limit cycles of period 2 (symmetric  $\mathbf{J}$ ) or 4 (when  $J_{ij} = -J_{ij}$ ). The reader is redirected to (Peretto, 1994, Section 3.2.4) for more details.

The asynchronous update rule can proceed in either of two ways: a random unit  $i$  is selected at each time step  $t$ , and then the rule Eq. (17) is applied (suitable for simulations); or neurons have a constant probability per unit time to be independently chosen for update at each instant  $t$  (suitable for direct hardware implementation).

The stopping condition for both approaches is similar. The iteration stops when the state of the network did not change between times  $t$  and  $t+1$ ; *i.e.* if  $\vec{\sigma}(t) = \vec{\sigma}(t+1) \equiv \vec{\sigma}^*$ . Thus, the network reached an *attractor*  $\vec{\sigma}^*$ . If we want to overload the network, we must account for  $P_{\text{err}}$ , giving the attractor some tolerance. So, we could impose that  $\vec{\sigma}(t+1) = \epsilon \vec{\sigma}(t) \approx \vec{\sigma}^*$ , where  $\epsilon \sim P_{\text{err}}$  is a small number.

Having attractors is what makes the network correct errors and associate error-prone or mixed inputs with a well-defined output. This is a consequence of the nonlinearity of  $F$ . If  $F$  were linear, then some linear combination of inputs, say  $0.3I_1 + 0.7I_2$ , would be mapped into a linear combination of outputs,  $0.3O_1 + 0.7O_2$ . However,

the step function forces the network into a *decision*. Usually, it converges to the nearest attractor, so iterating a Hopfield network under these conditions would probably lead to  $O_2$  (Hopfield, 1982).

### E. Extensions and biological relevance

There is a striking similarity between Eq. (17) and the equation of state for a magnet, Eq. (2). This is not a coincidence. At times, the update rule in Eq. (17) is referred to as being at zero temperature. This is because the solution to the mean-field Ising model at zero temperature is (Tragtenberg and Yokoi, 1995)  $m = \text{sign}(Jm + H)$ , which is related to the dynamics that we chose.

We can introduce noise in the dynamics via a temperature-like parameter. This requires replacing the sign function by the hyperbolic tangent, introducing the temperature (similarly to Eq. (2)), and switching to stochastic update rules (Hertz *et al.*, 1991; Hopfield, 1984; Peretto, 1994). The stochastic noise generated by small temperatures can optimize the convergence to the network memories. This is because small fluctuations can kick the network state out of local energy minima, by allowing sporadic random updates that increase the energy function. However, large temperatures make the dynamic too random, rendering the network useless in recalling memories. This is precisely the same behavior of a ferromagnet or a spin glass: increasing the temperature demagnetizes the system.

Other than the standard hyperbolic tangent,  $F$  can also be replaced by other functions with continuous-valued outputs. Importantly, the output has to be bounded within a range, so a typical sigmoid is recommended. Typical examples are  $F(x) = 1/(1 + e^{-x})$  (Hertz *et al.*, 1991), or  $F(x) = x/(1 + |x|)$  (Kinouchi and Kinouchi, 2010).

It can also be converted into a continuous-time evolution equation (Hopfield, 1984),

$$\tau_i \frac{d\sigma_i}{dt} = -\sigma_i + F \left( \sum_{j=1}^N W_{ij} \sigma_j(t) + H_i \right), \quad (24)$$

where  $\tau_i$  is the neuron's membrane time constant, or even (Hertz *et al.*, 1991),

$$\tau_i \frac{dh_i}{dt} = -h_i + H_i + \sum_{j=1}^N W_{ij} F(h_j), \quad (25)$$

where  $h_i$  is the effective local field on neuron  $i$ , Eq. (16). This results in the same attractor structure when the matrix  $\mathbf{W}$  is invertible (Pineda, 1988).

Importantly, the fact that the attractor dynamics works in these alternative models adds a higher degree of biological fidelity to the Hopfield idea (Fig 6). For

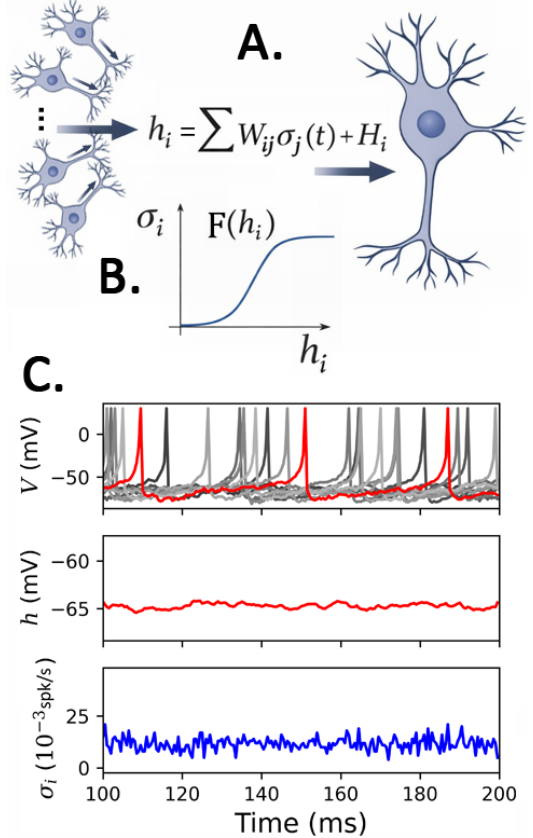


FIG. 6 **Continuous time and biological features.** **A.** Possible biological interpretation of the Hopfield dynamics, Eq. (17). Signals arriving from other neurons (also known as post-synaptic potentials) are integrated by the membrane of the receiving neuron (Dayan and Abbott, 2001; Gerstner *et al.*, 2014; Shimoura *et al.*, 2021).  $H_i$  represents the intrinsic dynamic of the receiving neuron membrane. This yields the effective field  $h_i(t)$ . **B.** The integrated signal generates an output firing rate in response. **C (top).** Membrane potential  $V$  of many neurons receiving noisy inputs, and generating spike events (action potentials). **C (middle).** The effective field  $h_i$  is the sum of all inputs with the intrinsic dynamics. So we can interpret it as the subthreshold signal in the membrane (meaning all except spikes). **C (bottom).** A neuron generates an output firing rate (number of spikes per unit time) by transducing its effective field. This is assumed to be constant in the Hopfield model, but it fluctuates in biological neurons.

example, Eq. (24) Eqs. (24) and (25) provide a natural biological interpretation of the Hopfield dynamics by moving from discrete-time, binary updates to continuous-time neuronal dynamics. In this formulation,  $\sigma_i(t)$  represents the activity of neuron  $i$ , interpreted as a firing rate or graded membrane potential rather than a binary state. The time constant  $\tau_i$  reflects the passive electrical properties of the neuronal membrane, while the nonlinear function  $F$  models the neuron's input–output relationship, accounting for thresholding and saturation effects observed in real neurons.

Equation (24) can be understood as a rate-based neu-

ron model, in which each neuron integrates synaptic inputs over time and relaxes toward a steady-state activity determined by the total synaptic drive and intrinsic dynamic  $H_i$ . Such rate models are widely used in theoretical neuroscience to describe population activity when precise spike timing is not essential (Gerstner *et al.*, 2014; Herz *et al.*, 2006).

Equation (25) offers an alternative but closely related description, in which the dynamical variable is the local field  $h_i$ , rather than the output activity  $\sigma_i$  itself. In this case, the neuron integrates inputs into an internal state variable, which is then transformed into an output firing rate by the nonlinear function  $F$ . This separation between integration and output mirrors the biological distinction between membrane potential dynamics and spike generation, and constitutes the conceptual basis of integrate-and-fire neuron models (Gerstner *et al.*, 2014; Shimoura *et al.*, 2021). These models are so powerful that they can reliably reduce the dimensionality of the membrane dynamics while capturing many relevant of over 600 neurons (Teeter *et al.*, 2018), including those directly involved in spatial memory, such as mossy cells (Trinh *et al.*, 2023).

While the original Hopfield model assumes that the synaptic weights  $W_{ij}$  are fixed by some convenient definition, biological networks continuously modify their synapses through activity-dependent plasticity. A particularly important mechanism is spike-timing-dependent plasticity (STDP), in which the change in  $W_{ij}$  depends on the relative timing of presynaptic (input neurons) and postsynaptic (receiving neuron) spikes. Experiments in hippocampal and cortical slices have shown that synapses are strengthened when presynaptic firing precedes postsynaptic firing, and weakened in the opposite case (Markram and Tsodyks, 1996). Such rules naturally implement a temporally refined version of Hebbian learning and provide a biologically realistic way to build the effective  $W_{ij}$  “on the fly” from ongoing neuronal activity.

This shows that even though associative memory relies on idealized binary neurons or synchronous updates using a constructed interaction matrix, it can emerge robustly from biological neurons in our brains. More generally, these equations support the view that cortical memory and computation can be understood as dynamical processes unfolding in high-dimensional neural state space, where memories correspond to stable attractors and cognitive processes correspond to trajectories between them. This perspective has influenced a wide range of biological theories, from models of working memory and pattern completion to modern recurrent neural network architectures (Rolls and Treves, 1999, 2024).

## IV. BRINGING THE HOPFIELD MODEL TO THE PHYSICS CLASSROOM

Now, we give examples that can be easily approached in undergraduate classes. We presented the model with enough details to give instructors a complete background when bringing up these problems. They go from raw mathematical exercises to implementing computer simulations, and using it to probe for different behaviors of the system.

### A. Examples in Computational Physics

The most direct application of the Hopfield model is when teaching computational methods in physics. The basic Hopfield model theory is deterministic so it should be easier to grasp than, for example, the Metropolis MC algorithm. Even though it could also be a stepping stone for more complex stochastic simulations. In fact, many systems in physics can be simulated very similarly to the Hopfield model, with some particular modifications for each case. This includes the contact process (de Oliveira and Dickman, 2005; Girardi-Schappo, 2025; Henkel *et al.*, 2008; Marro and Dickman, 1999) different algorithms for MC simulations (Newman and Barkema, 1999), and even more complex biologically-motivated neural network simulators (Gewaltig and Diesmann, 2007; Shimoura *et al.*, 2021).

In this paper, we give enough details so that anyone can implement their own simulation. We also made our code freely available (Girardi-Schappo *et al.*, 2025). The implementation of a basic Hopfield network from the scratch can be a standalone whole-term project to give students. Alternatively, instructors could also give part of the code and ask for particular studies or modifications.

In both cases, this emulates the daily affairs of research involving computational physics. Here are some problems that can be proposed, once students have a working code:

- *Example Problem A.1. Identifying attractors.* Create a network of  $N = 100$  neurons and store three memories,  $\{\vec{\xi}^{(1)}, \vec{\xi}^{(2)}, \vec{\xi}^{(3)}\}$ . Make sure the memories are reasonably uncorrelated, i.e.,  $M(\vec{\xi}^{(\mu)}, \vec{\xi}^{(\nu)}) \approx 0$ , and easily distinguishable by visual inspection (e.g., you can use patterns such as “H”, “X” and “#”). Take the first memory  $\vec{\xi}^{(1)}$ , flip a fraction  $\alpha$  of its neurons and use it as initial condition for the dynamics. Study the convergence of the network to  $\vec{\xi}^{(1)}$  as  $\alpha$  is increased from 0 to 1 in steps of 0.1. At what  $\alpha_c$  does the convergence become unreliable? Repeat the study using  $\vec{\xi}^{(2)}$  and  $\vec{\xi}^{(3)}$ . Are the  $\alpha_c$  for each memory equal?

To flip a fraction  $\alpha$  of the memory state, we can construct an identity-like matrix  $\eta$  where a random fraction  $\alpha$  of its diagonal entries are  $-1$ . Then,  $\vec{\sigma}(0) = \eta \vec{\xi}^{(1)}$

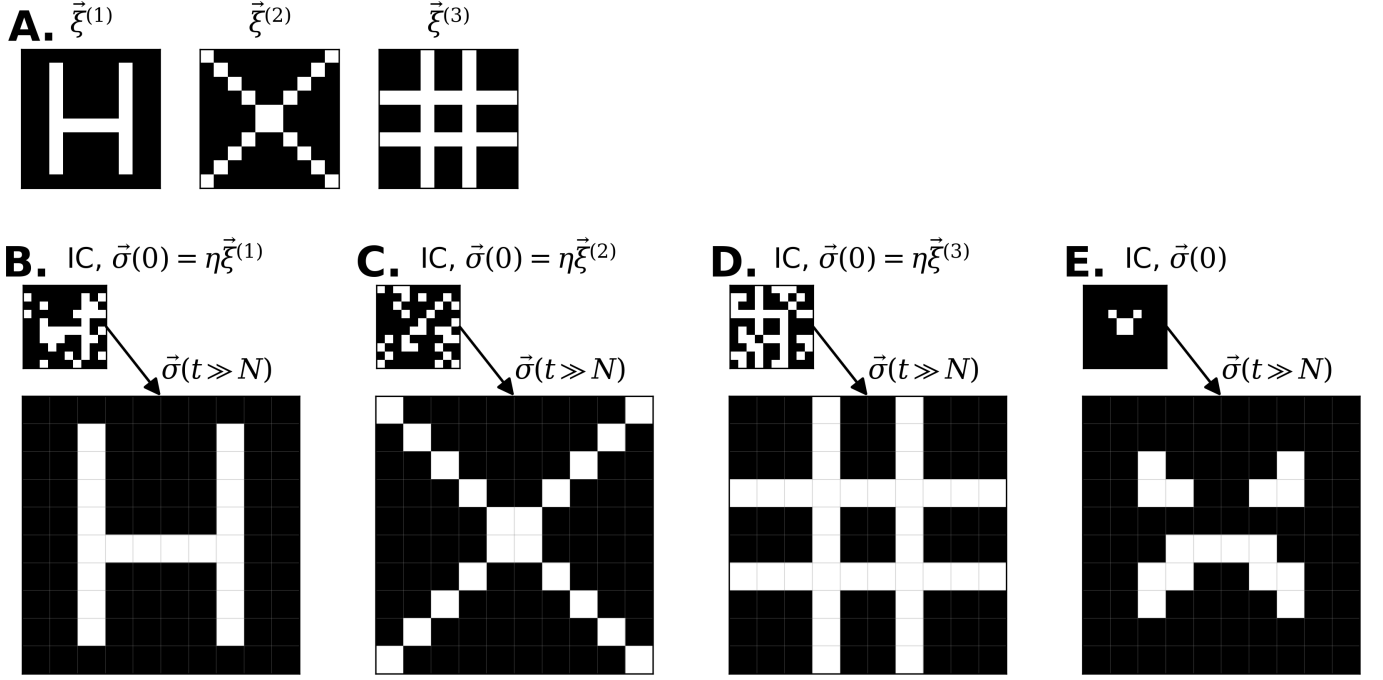


FIG. 7 **Network attractors with three memories.** Network with  $N = 100$  neurons; states are displayed using the convention established in Fig. 3A. **A.** Patterns stored in the connectivity matrix  $\mathbf{W}$  using Eq. (11). **B, C, D.** ICs are the memory patterns with  $\alpha = 20\%$  of their neurons randomly flipped (top); the attractor reached after iterating Eq. (17) either synchronously or asynchronously matches the corresponding memory used as IC (bottom). **E.** A specific IC (top) led to a spurious attractor (hallucination) after asynchronously iterating through 10 MC steps.

can be used as the initial condition. An example of the output for  $\alpha = 0.2$  is shown in Fig. 7A,B,C,D.

A suggestion is to fix the seed of the random number generator before running any the analysis proposed in each problem, so that results are reproducible. It is also better to use asynchronous updates, since convergence is guaranteed below storage capacity.

Direct follow-up problems can be stated:

- *Example Problem A.2. Antimemories.* Repeat the previous problem starting from the flipped memories,  $-\vec{\xi}^{(1)}$ ,  $-\vec{\xi}^{(2)}$ , and  $-\vec{\xi}^{(3)}$ , with a fraction  $\alpha$  of neurons reversed. Does the network converge to the corresponding attractor  $\vec{\xi}$  or to its flipped versions,  $-\vec{\xi}$ ?

This is just a simple exercise to show that flipped attractors are also valid memories (e.g., Fig. 8C).

- *Example Problem A.3. Spurious memories.* During the exploration of initial conditions in Problem A.1, did you find an attractor that was not in the set of memories,  $\{\vec{\xi}^{(1)}, \vec{\xi}^{(2)}, \vec{\xi}^{(3)}\}$ ? If so, report the  $\alpha$  values where this happened. Construct initial conditions by mixing parts of two or more memories so that the network converges to these spurious attractors.

Spurious attractors can be found by either asynchronous (Fig. 7E) or synchronous (Fig. 8B) dynamics.

- *Example Problem A.4. Overlap over time.* Consider the code for memory retrieval from an initial condition using asynchronous updates (Appendix A). Modify it to calculate and also return the overlap of the network state  $\vec{\sigma}(t)$  with every memory  $\vec{\xi}^{(\mu)}$  at every time step,

$M(\vec{\sigma}(t), \vec{\xi}^{(\mu)})$ . Plot all the overlaps versus the time step for a network with  $N = 100$  neurons and three memories. Using this plot, repeat Problems A.1, A.2 and A.3 with fixed  $\alpha = 0.2$ . It is easier to track the convergence by the overlap than by visual inspection. Report the value of the overlap for when the network converged to a memory, an antimemory, or a spurious attractor.

The code is given in Appendix A for reference, together with the function for storing memories in the matrix  $\mathbf{W}$ . One solution for this problem is in our code repository (Girardi-Schappo *et al.*, 2025), in the function “iterate\_hopfield\_sequential”. An example of what can be seen in each situation is shown in Fig. 9: memories converge to  $M = +1$ , antimemories converge to  $M = -1$ , and spurious attractors converge to something in between.

- *Example Problem A.5. Energy dynamics.* Modify the provided code (Appendix A) to calculate and return the energy function of the system at every time step. Note that all thresholds are zero. Create a network with  $N = 100$  neurons with two memories,  $\{\vec{\xi}^{(1)}, \vec{\xi}^{(2)}\}$ . When represented on the lattice (Fig. 3A),  $\vec{\xi}^{(1)}$  must be vertical stripes (first stripe in the left is  $-1$ , second is  $+1$ , etc), and  $\vec{\xi}^{(2)}$  must be horizontal stripes (first stripe from the top is  $+1$ , second is  $-1$ , etc). The overlap between these memories is zero. As initial condition, use the whole network set to  $-1$ , except for the first two vertical stripes of memory  $\vec{\xi}^{(1)}$ . Run the dynamics and record the energy

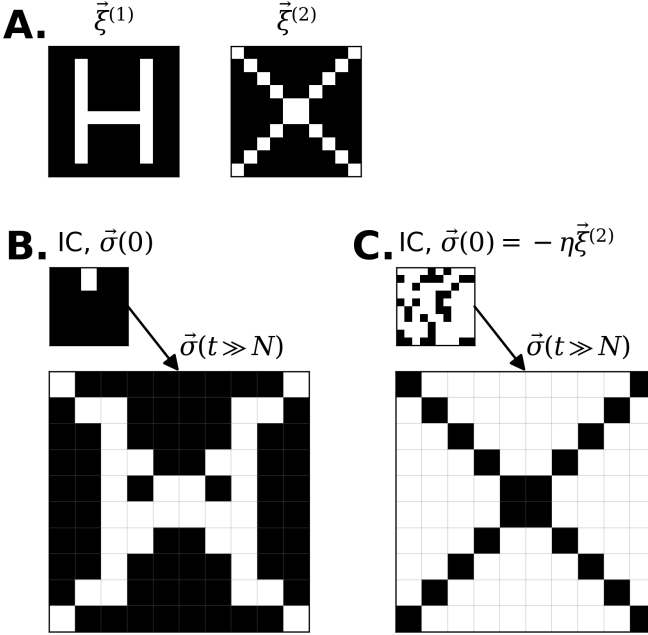


FIG. 8 **Hallucinations and antimemory.** Network with  $N = 100$  neurons and two stored memories; states are displayed using the convention established in Fig. 3A. **A.** Patterns stored in the connectivity matrix  $\mathbf{W}$  using Eq. (11). **B.** A specific IC (top) led to a spurious attractor (hallucination) after synchronously iterating through 15 steps. **C.** IC was the flipped “X” pattern with  $\alpha = 30\%$  of its neurons randomly flipped (top); the attractor reached after iterating Eq. (17) either synchronously or asynchronously matches the flipped memory used as IC (bottom).

as a function of time. Do the same for  $\vec{\xi}^{(2)}$ , but with an initial condition set to  $+1$ , except for the first two horizontal stripes of  $\vec{\xi}^{(2)}$ . Compare the evolution of the energy of these two patterns. Can you tell apart both patterns by the energy? Why?

Both patterns have the same energy, since they both have the same number of activated and deactivated neurons. Thus, it is not possible to distinguish between both patterns only by looking at the energy plot, even if both patterns are completely uncorrelated. For example, in Fig. 10 we show the evolution of the energy of the network while retrieving the patterns from Fig. 7 and 8. The “X” and “H” patterns have the same energy.

- *Example Problem A.6. Memory capacity.* The storage capacity of a network is about 13.8% of  $N$ . Create a network with  $N = 100$  neurons. Add ten random memories and run the dynamics from a few initial conditions. Use the energy and overlap plots to tell whether the dynamics converged to a memory (convergence requires that the overlap is  $M = \pm 1$  between some memory and the final network state). Now, add ten more random memories, run the dynamics again from another handful of initial conditions, and check convergence from the energy and overlap plots. How does this plot compare with the first one? Keep adding more memories and checking the overlap and memory plots. Is the network stable?

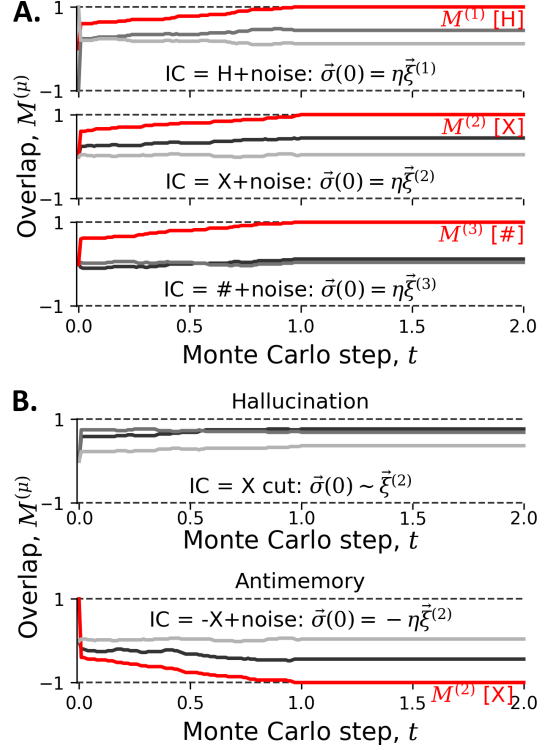


FIG. 9 **Overlap of network state and memories during the dynamics.** **A.** The overlap goes to  $M = +1$  when the network converges to one of the memories  $\vec{\xi}^{(\mu)}$ ; ICs and attractors are in Fig. 7. **B.** The overlap goes to  $M = -1$  when the network converges to an antimemory  $-\vec{\xi}^{(\mu)}$  (bottom), or stays trapped within  $(-1, 1)$  when the network converges to an spurious attractor (top); ICs and attractors are in Fig. 8.

The network becomes saturated as more memories are added. Eventually, unstable patterns can emerge, and avalanches of neurons flipping their states can happen.

Other problems can ask to compare synchronous with asynchronous dynamics, change the transfer function  $F$  and implement thresholds. Again, this can be done systematically comparing with previous results from the above problems. This routine not only invites students to reflect on the Hopfield model, but also emulates how research work is carried out.

## B. Examples in Dynamical Systems

The convergence and stability problems presented in Section III can be discussed in nonlinear dynamics courses.

- *Example Problem B.1.* Consider a network of  $N$  neurons with  $P = 1$  memory. Representing the network state as a column vector, show that the memory  $\vec{\xi}$  is an attractor if  $H_i \in (-1, 1)$ .

This was solved in Eq. (20). With vectors, we can define the local field column vector as  $\vec{h}(t) = \mathbf{W}\vec{\sigma}(t) + \vec{H}$ , such that  $\vec{\sigma}(t+1) = F(\vec{h}(t))$  is a sign function that acts

componentwise,  $\vec{H}$  is a column vector with the threshold for each neuron, and  $\mathbf{W}$  is given by Eq. (28).

Taking  $\vec{\sigma}(t) = \vec{\xi}$ , we need to retrieve it through a single iteration,

$$\begin{aligned}\vec{\sigma}(t+1) &= F(\vec{h}(t)) = F(\mathbf{W}\vec{\xi} + \vec{H}) \\ &= F\left(\frac{1}{N}\vec{\xi}\vec{\xi}^T\vec{\xi} + \vec{H}\right) \\ &= F\left(\vec{\xi} + \vec{H}\right),\end{aligned}\quad (26)$$

where we used the overlap definition as the scalar product,

$$NM(\vec{\xi}, \vec{\xi}) = \vec{\xi}^T \vec{\xi} = N.$$

Recalling that  $\xi_i = \pm 1$ , Eq. (26) evaluates to

$$F(\xi_i + H_i) = \begin{cases} +1 & \text{if } \xi_i \geq -H_i \\ -1 & \text{if } \xi_i < -H_i \end{cases} = \xi_i,$$

since  $\xi_i = +1 > -H_i$  and  $\xi_i = -1 < -H_i$  for  $H_i \in (-1, 1)$ .

• *Example Problem B.2.* Consider a network of  $N$  neurons with  $P$  memories and all thresholds  $H_i = 0$ . Representing the network state as a column vector, show that the memory  $\vec{\xi}^{(\nu)}$  is an attractor if  $M(\vec{\xi}^{(\mu)}, \vec{\xi}^{(\nu)}) \approx 0$ , i.e. the overlap (or correlation) between memory  $\nu$  and any other memory is negligible.

This was done when deriving Eq. (21). Similarly to the previous case, we just need to evaluate the local field  $\vec{h}(t)$  applied to the state  $\vec{\sigma}(t) = \vec{\xi}^{(\nu)}$ ,

$$\begin{aligned}\vec{\sigma}(t+1) &= F(\vec{h}(t)) = F(\mathbf{W}\vec{\xi}^{(\nu)}) \\ &= F\left(\frac{1}{N} \sum_{\mu=1}^P \vec{\xi}^{(\mu)} (\vec{\xi}^{(\mu)})^T \vec{\xi}^{(\nu)}\right) \\ &= F\left(\frac{1}{N} \vec{\xi}^{(\nu)} (\vec{\xi}^{(\nu)})^T \vec{\xi}^{(\nu)} + \sum_{\substack{\mu=1 \\ \mu \neq \nu}}^P \vec{\xi}^{(\mu)} \left(\frac{1}{N} (\vec{\xi}^{(\mu)})^T \vec{\xi}^{(\nu)}\right)\right) \\ &= F\left(\vec{\xi}^{(\nu)} + \sum_{\substack{\mu=1 \\ \mu \neq \nu}}^P \vec{\xi}^{(\mu)} M(\vec{\xi}^{(\mu)}, \vec{\xi}^{(\nu)})\right).\end{aligned}\quad (27)$$

When  $|M(\vec{\xi}^{(\mu)}, \vec{\xi}^{(\nu)})| < \frac{\epsilon}{P} \ll 1$  for all  $\mu \neq \nu$ , and  $0 < \epsilon < 1$ , then Eq. (27) evaluates to  $\vec{\sigma}(t+1) = F(\vec{\xi}^{(\nu)} + \mathcal{O}[\epsilon]) = \vec{\xi}^{(\nu)}$ . Since  $\vec{\xi}^{(\nu)}$  is retrieved in one iteration, it is an attractor of the dynamics.

Similarly, the basins of attraction based on the Hamiltonian naturally emerges from the convergence study in Section IV.A. These computational problems can also be proposed, depending on the intended nature of the

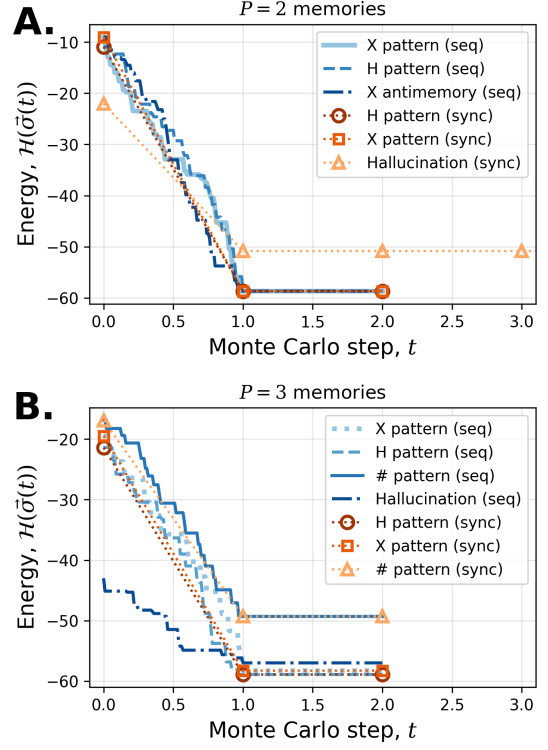


FIG. 10 **Evolution of the network energy function.** Network with  $N = 100$  neurons. **A.** Energy as function of time for each condition in Fig. 8. **B.** Energy as function of time for each condition in Fig. 7. Hallucinations (attractors that were not purposefully encoded in the Hamiltonian) are evidence of local minima.

course. We presented in Fig. 5 a way to sort the network states that reveals the wells in the energy function, each of which is directly analogous to the basin for each attractor.

### C. Examples in Linear Algebra

Linear algebra is often one of the first mathematical tools encountered by undergraduate physics students, yet its role in research models is not always immediately apparent. Concepts such as vectors, dot products, and matrices are typically taught in abstract settings or applied to canonical examples like rotations and eigenvalue problems. In the Hopfield model, encoding and recalling information use vector operations and are naturally represented as matrices. Thus, the problems given in Section IV.B can also be brought to Linear Algebra classes. Another example is the following:

• *Example Problem C.1.* Show that the weights, Eq. (11), form a symmetric matrix given by the sum of external products between the memory states  $\vec{\xi}^{(\mu)}$ , each of which is written as a column vector.

This problem can be introduced by the instructor talking about the importance of vector and matrix algebra in artificial intelligence. Then, the instructor can derive the  $W_{ij}$  from Eq. (9) and (10), and ask students to make

this simple demonstration,

$$\begin{aligned}
 \mathbf{W} &= \frac{1}{N} \begin{bmatrix} \sum_{\mu=1}^P \xi_1^{(\mu)} \xi_1^{(\mu)} & \sum_{\mu=1}^P \xi_1^{(\mu)} \xi_2^{(\mu)} & \dots & \sum_{\mu=1}^P \xi_1^{(\mu)} \xi_N^{(\mu)} \\ \sum_{\mu=1}^P \xi_2^{(\mu)} \xi_1^{(\mu)} & \sum_{\mu=1}^P \xi_2^{(\mu)} \xi_2^{(\mu)} & \dots & \sum_{\mu=1}^P \xi_2^{(\mu)} \xi_N^{(\mu)} \\ \vdots & \vdots & \ddots & \vdots \\ \sum_{\mu=1}^P \xi_N^{(\mu)} \xi_1^{(\mu)} & \sum_{\mu=1}^P \xi_N^{(\mu)} \xi_2^{(\mu)} & \dots & \sum_{\mu=1}^P \xi_N^{(\mu)} \xi_N^{(\mu)} \end{bmatrix} \\
 &= \frac{1}{N} \sum_{\mu=1}^P \begin{bmatrix} \xi_1^{(\mu)} \xi_1^{(\mu)} & \xi_1^{(\mu)} \xi_2^{(\mu)} & \dots & \xi_1^{(\mu)} \xi_N^{(\mu)} \\ \xi_2^{(\mu)} \xi_1^{(\mu)} & \xi_2^{(\mu)} \xi_2^{(\mu)} & \dots & \xi_2^{(\mu)} \xi_N^{(\mu)} \\ \vdots & \vdots & \ddots & \vdots \\ \xi_N^{(\mu)} \xi_1^{(\mu)} & \xi_N^{(\mu)} \xi_2^{(\mu)} & \dots & \xi_N^{(\mu)} \xi_N^{(\mu)} \end{bmatrix} \\
 &= \frac{1}{N} \sum_{\mu=1}^P \tilde{\xi}^{(\mu)} \left( \tilde{\xi}^{(\mu)} \right)^T. \tag{28}
 \end{aligned}$$

Symmetry follows from the commutativity of the multiplication between  $\xi_i^{(\mu)}$  and  $\xi_j^{(\mu)}$ .

A follow-up question can deal with the retrieval and stability of memories, treating the memory states as vectors and the couplings as a matrix.

#### D. Examples in Statistical Physics

Even though the fundamental principles of the Hopfield model directly derive from the base ideas of statistical mechanics, it is not easy to make a direct connection in a typical undergraduate course. At this level, we are usually interested in deriving equilibrium thermodynamics from statistical principles through the ensemble theory.

Some analogies can be made as motivations, allowing students to recognize objects from statistical physics in an applied setting. The Hamiltonian of the Hopfield model is written in the same form encountered in equilibrium statistical mechanics, and the role of temperature is analogous to thermal noise in spin systems. Large temperatures demagnetize magnets, and make Hopfield networks become unstable, yielding just random configurations. So the magnetic phase transition into a paramagnet state appears in both systems.

Students who have learned to interpret free energy curves and equilibrium states in the Ising model (Fig. 1) can apply exactly the same reasoning to understand how a neural network stores and retrieves information (Fig. 11), without introducing new formal definitions. The Hopfield model thus serves as a bridge between abstract thermodynamic principles and a modern applied problem in neural computation.

#### V. CONCLUDING REMARKS

The recent rise of AI is steadily reshaping both scientific practice and the classroom. Rather than replacing

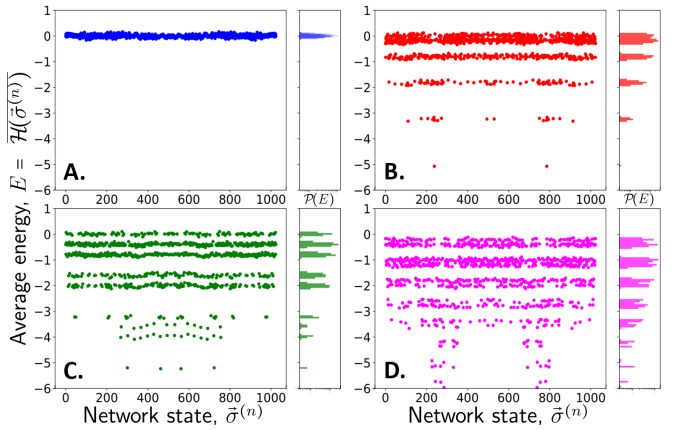


FIG. 11 **Average energy landscape for the Hopfield model with memory.** The plots show the average energy taken over 1000 realizations of the interaction matrix  $\mathbf{W}_{\text{eff}}$  for every  $\vec{\sigma}^{(n)}$  state in a network with  $N = 10$  neurons.  $\mathbf{W}_{\text{eff}} = \mathbf{W}_{\text{rand}} + \mathbf{W}$ , where  $\mathbf{W}_{\text{rand}}$  is a random matrix with Gaussian distributed elements with zero mean and unity standard deviation, and  $\mathbf{W}$  is the Hebbian matrix, Eq. (11). The storage capacity is just around one memory (for absolutely stable attractors). **A.**  $\mathbf{W}_{\text{eff}}$  is only given by the random part (no memory stored); this is equivalent to the spin glass average energy in Fig. 2. **B.** Only a single memory  $\vec{\xi}$  is encoded in  $\mathbf{W}$ . It is the same memory for every realization of  $\mathbf{W}_{\text{eff}}$ . The two minima in  $\mathcal{H}$  correspond to  $\vec{\xi}$  and  $-\vec{\xi}$ . The energy levels that arise reflect the discrete nature of the Hamiltonian. **C.** The same two memories are encoded in  $\mathbf{W}$  for every  $\mathbf{W}_{\text{eff}}$ . More energy levels appear, since the network is already above the stable storage capacity. **D.** The same three memories are encoded in  $\mathbf{W}$  for every  $\mathbf{W}_{\text{eff}}$ . Many energy levels are now present, making local minima that can trap the dynamics into hallucinations. The averaging smoothens the random fluctuations and make the minima due to the Hebbian part apparent.

traditional training, it highlights the need for deeper engagement with the tools that now mediate much of our work. Future physicists will be expected not only to use computational and AI-based methods, but to understand their foundations, limitations, and domains of applicability, so they can adapt and extend them when necessary.

To this extent, the Hopfield model provides a direct link between simple physics concepts and modern AI. Some examples of real-world problems that can be solved with these networks are: scheduling of truck deliveries or flights, the automatic movement of drills or robot arms, the design of chips with minimal wiring, etc. These can be mapped on combinatorial problems, such as the traveling salesman (minimizing traveled distance), or graph bipartite (splitting a graph in two parts connected by the minimum amount of edges). To solve them, we can define cost functions that can be directly mapped on the Hopfield Hamiltonian, from where the connection weights and thresholds are easily inferred. Then, the energy-minimization dynamics naturally leads to near-optimal solutions.

This shows that physicists can contribute essential in-

sight to the understanding and development of AI systems through our common knowledge of energy landscapes, stability, and collective behavior. In a society increasingly reliant on intelligent algorithms for industry and decision-making, this can make a difference for finding jobs in contemporary society.

This calls for a gradual update of standard curricula, incorporating contemporary problems where physics, data analysis, and learning algorithms naturally converge. Embedding core concepts in such contexts can help ensure that students develop lasting understanding and critical judgment, preparing them to work thoughtfully with the evolving technologies of their field.

## DATA AVAILABILITY STATEMENT

Simulations will be freely available in an online repository (Girardi-Schappo *et al.*, 2025)

<https://github.com/neuro-physics/hopfield-neural-network>.

## AUTHOR DECLARATIONS AND CONTRIBUTIONS

The authors declare no competing interests.

Author contributions removed due to double-blind peer review. D.D.C. and M.H. ran simulations and performed calculations. C.F.V. performed calculations. M.G.-S. performed calculations, proposed, and supervised the work. All authors wrote the manuscript.

## ACKNOWLEDGMENTS

M.G.-S. thanks financial support from Fundação de Amparo a Pesquisa e Inovação do Estado de Santa Catarina (FAPESC), Edital 21/2024 (Grant n. 2024TR002507) and from Conselho Nacional de Desenvolvimento Científico e Tecnológico (CNPq Grant n. 302102/2025-6). This research is supported by INCT-NeuroComp (CNPq Grant 408389/2024-9). D.D.C. and M.H. thank partial financial support by CNPq-Brazil, and C.F.V. thanks partial financial support from CAPES-Brazil.

## REFERENCES

Ackley, David H, Geoffrey E. Hinton, and Terrence J. Sejnowski (1985), “A learning algorithm for boltzmann machines,” *Cognitive Science* **9**, 147–169.

Carneiro, C.EI, V.B. Henriques, and S.R. Salinas (1989), “On the equivalence of different Landau expansions,” *Physica A* **162**, 88–98.

Dayan, P, and L F Abbott (2001), *Theoretical Neuroscience* (The MIT Press, Cambridge, MA, USA).

de Oliveira, Marcelo Martins, and Ronald Dickman (2005), “How to simulate the quasistationary state,” *Phys. Rev. E* **71**, 016129.

Derrida, Bernard (1980), “Random-energy model: limit of a family of disordered models,” *Phys. Rev. Lett.* **45**, 79–82.

Edwards, S F, and P W Anderson (1975), “Theory of spin glasses,” *Journal of Physics F: Metal Physics* **5**, 965.

Gerstner, Wulfram, Werner M. Kistler, Richard Naud, and Liam Paninski (2014), *Neuronal Dynamics* (Cambridge University Press, New York USA).

Gewaltig, M, and M. Diesmann (2007), “NEST (NEural Simulation Tool),” *Scholarpedia* **2**, 1430.

Girardi-Schappo, M, MHR Tragtenberg, and O Kinouchi (2013), “A brief history of excitable map-based neurons and neural networks,” *J. Neurosci. Methods* **220** (2), 116–130.

Girardi-Schappo, Mauricio (2025), “Contact Process Simulation,” <https://github.com/neuro-physics/contact-process>, Accessed: 29 December 2025.

Girardi-Schappo, Mauricio, Denis D. Capriotti, and Matheus Haas (2025), “Hopfield Neural Network Simulation,” <https://github.com/neuro-physics/hopfield-neural-network>, Accessed: 29 December 2025.

Hebb, D O (1942), *The Organization of Behavior* (John Wiley & Sons, New York, NY, USA).

Henkel, Malte, Haye Hinrichsen, and Sven Lübeck (2008), *Non-Equilibrium Phase Transitions* (Springer, Dordrecht, The Netherlands).

Hertz, J, A Krogh, and R G Palmer (1991), *Introduction to the Theory of Neural Computation* (Addison-Wesley Publishing Company, Boston, MA, USA).

Herz, Andreas V M, Tim Gollisch, Christian K. Machens, and Dieter Jaeger (2006), “Modeling single-neuron dynamics and computations: A balance of detail and abstraction,” *Science* **314**, 80–85.

Hinton, G E, and T. J. Sejnowski (1983), “Optimal perceptual inference,” in *Proceedings of the IEEE conference on Computer Vision and Pattern Recognition* (IEEE, Washington DC, USA) pp. 448–453.

Hopfield, J J (1982), “Neural networks and physical systems with emergent collective computational abilities,” *Proc. Nat. Acad. Sci. (USA)* **79**, 2554–2558.

Hopfield, J J (1984), “Neurons with graded response have collective computational properties like those of two-state neurons,” *Proc. Nat. Acad. Sci. (USA)* **81**, 3088–3092.

Hopfield, J J, and D. W. Tank (1985), ““Neural” computation of decisions in optimization problems,” *Biological Cybernetics* **52**, 141–152.

Hopfield, John J, and David W. Tank (1986), “Computing with neural circuits: A model,” *Science* **233**, 625–633.

Kinouchi, O, and R R Kinouchi (2010), “Dreams, endocannabinoids and itinerant dynamics in neural networks: re elaborating crick-mitchison unlearning hypothesis,” arXiv:cond-mat/0208590 [cond-mat.dis-nn].

Markram, Henry, and Misha Tsodyks (1996), “Redistribution of synaptic efficacy between neocortical pyramidal neurons,” *Nature* **382**, 807–810.

Marro, J, and R. Dickman (1999), *Nonequilibrium Phase Transitions in Lattice Models* (Cambridge University Press, Cambridge, UK).

McCulloch, W S, and W H Pitts (1943), “A logical calculus of the ideas immanent in nervous activity,” *Bull. Math. Biophys.* **5**, 115–133.

Mézard, M, G. Parisi, N. Sourlas, G. Toulouse, and M. Virasoro (1984), “Nature of the spin-glass phase,” *Phys. Rev.*

Lett. **52**, 1156–1159.

Mézard, Marc, Giorgio Parisi, and Miguel Angel Virasoro (1987), *Spin glass theory and beyond* (World Scientific, Singapore).

Newman, M E J, and G T Barkema (1999), *Monte Carlo Methods in Statistical Physics* (Oxford University Press, New York, USA).

Nishimori, Hidetoshi (2001), *Statistical Physics of Spin Glasses and Information Processing: An Introduction* (Oxford University Press, New York, NY, USA).

Nobel Prize Outreach, (2024), “All Nobel Prizes 2024,” <https://www.nobelprize.org/all-nobel-prizes-2024/>, Accessed: 29 December 2025.

Peretto, P (1994), *An Introduction to the Modeling of Neural Networks* (Cambridge University Press, Cambridge, UK).

Pineda, Fernando J (1988), “Dynamics and architecture for neural computation,” *Journal of Complexity* **4**, 216–245.

Rojas, Raúl (1996), *Neural networks: a systematic introduction* (Springer-Verlag, Berlin, Germany).

Rolls, Edmund T, and Alessandro Treves (1999), *Neural Networks and Brain Function* (Oxford University Press, New York, NY, USA).

Rolls, Edmund T, and Alessandro Treves (2024), “A theory of hippocampal function: New developments,” *Progress in Neurobiology* **238**, 102636.

Ruelle, David (1987), “A mathematical reformulation of derrida’s REM and GREM,” *Communications in Mathematical Physics* **108**, 225–239.

Salinas, Silvio R A (2001), *Introduction to Statistical Physics* (Springer, New York, NY, USA).

Sherrington, David, and Scott Kirkpatrick (1975), “Solvable model of a spin-glass,” *Phys. Rev. Lett.* **35**, 1792–1796.

Shimoura, Renan O, Rodrigo F. O. Pena, Vinicius Lima, Nilton L. Kamiji, Mauricio Girardi-Schappo, and Antonio C. Roque (2021), “Building a model of the brain: from detailed connectivity maps to network organization,” *Eur. Phys. J. Spec. Top.* **230**, 2887–2909.

Strogatz, S H (2024), *Nonlinear Dynamics and Chaos: With Applications to Physics, Biology, Chemistry, and Engineering. 3rd edition* (CRC Press).

Teeter, Corinne, Ramakrishnan Iyer, Vilas Menon, Nathan Gouwens, David Feng, Jim Berg, Aaron Szafer, Nicholas Cain, Hongkui Zeng, Michael Hawrylycz, Christof Koch, and Stefan Mihalas (2018), “Generalized leaky integrate-and-fire models classify multiple neuron types,” *Nat Comm* **9**, 709.

Tomé, Tânia, and Mário J. Oliveira (2015), *Stochastic Dynamics and Irreversibility* (Springer International Publishing, Switzerland).

Tragtenberg, M H R, and C S O Yokoi (1995), “Field behavior of an Ising model with competing interactions on the Bethe lattice,” *Phys. Rev. E* **52(3)**, 2187–2197.

Trinh, Anh-Tuan, Mauricio Girardi-Schappo, Jean-Claude Béïque, André Longtin, and Leonard Maler (2023), “Adaptive spike threshold dynamics associated with sparse spiking of hilar mossy cells are captured by a simple model,” *J Physiol* **601**, 4397–4422.

## Appendix A: Simple python code for storage and retrieval of memory

Here is a python 3.8.2 implementation of the Hopfield Hebbian-like storage and retrieval algorithm. This implementation depends only on numpy 1.24.4 (imported using “import numpy as np”). More details on the code repository (function names were changed for clarity) (Girardi-Schappo *et al.*, 2025).

- Storage:

```
def store_patterns(patterns):
    """
    Parameters
    -----
    patterns : array-like or list of numpy.ndarray
        A collection of reference patterns used to train
        the Hopfield network.
        Each pattern should be a 1D array of length N (
        flattened vector).
        Values are typically +1 or -1.
    Returns
    -----
    W : numpy.ndarray
        The weight matrix of shape (N, N), initialized
        according to Hebbian learning.
    """
    patterns = np.atleast_2d(patterns)
    N = len(patterns[0])
    W = np.zeros((N, N))
    for xi in patterns:
        W += np.outer(xi, xi) / N
    np.fill_diagonal(W, 0)
    return W
```

- Retrieval:

```
def get_memory_async(W, s0, max_MCsteps):
    """
    Parameters
    -----
    W : numpy.ndarray
        Symmetric weight matrix of shape (N, N), where N
        is the number of neurons.
    s0 : numpy.ndarray
        Initial state vector of shape (N,), with entries
        typically +1 or -1.
    max_MCsteps : int, optional (default=10)
        Maximum number of Monte Carlo steps (epochs). Each
        step updates all neurons once.
    Returns
    -----
    s : numpy.ndarray
        Final state vector after convergence or reaching ‘
        max_MCsteps’.
    """
    # the number of neurons
    N = len(s0)
    # vector containing the index of each neuron
    indices = np.arange(N)
    # copy of the initial state vector
    s = s0.copy().astype(float)
    # main time loop
    # t_MC = 1 MC step = 1 epoch = N time steps
    for t_MC in range(1, max_MCsteps):
        # Randomize neuron update order
        np.random.shuffle(indices)
        # flag to keep track of the network state
        state_changed = False
        # try to update every neuron
        for i in indices:
            # Calculate the local field for neuron i
            h_i      = np.dot(W[i, :], s)
            # new state of neuron i
            s_i_new = 1.0 if h_i >= 0 else -1.0
            # if the state of neuron i changed
            if s_i_new != s[i]:
                # keep the new state
                s[i] = s_i_new
                # update network state flag
                state_changed = True
            # no neurons changed state during a full pass,
            # we hit a local minimum
            # so we exit and return the retrieved pattern
            if not state_changed:
                break
    return s
```